A STUDY ON CONTROL LAW AND HARDWARE APPLYING TO FLEXIBLE CONTROL ROTOR BLADES FOR FLIGHT PERFORMANCE IMPROVEMENT

Takahiro Noda, noda_takahiro@khi.co.jp, Kawasaki Heavy Industries, Ltd. (Japan)
Tomoka Tsujiuchi, tsujiuchi_tomoka@khi.co.jp, Kawasaki Heavy Industries, Ltd. (Japan)
Harufumi Yoneda, yoneda_harufumi@khi.co.jp, Kawasaki Heavy Industries, Ltd. (Japan)
Shigeru Tobari, tobari_s@khi.co.jp, Kawasaki Heavy Industries, Ltd. (Japan)
Itsuhiko Kaneshige, kaneshige_itsuhiko@khi.co.jp, Kawasaki Heavy Industries, Ltd. (Japan)
Taisuke Somekawa, somekawa_taisuke@khi.co.jp, Kawasaki Heavy Industries, Ltd. (Japan)
Noboru Kobiki, kobiki.noboru@jaxa.jp, Japan Aerospace Exploration Agency (Japan)
Yasutada Tanabe, tanabe.yasutada@jaxa.jp, Japan Aerospace Exploration Agency (Japan)

Abstract
Flexible control systems for helicopter blades (e.g. HHC, IBC, Active Twist and Active Flap) have the potential to improve flight performances of rotorcraft. This study selects Active Flap as the flexible control system because it is more feasible than the others and it has been abundantly experienced in author's organizations. CAMRAD II analyses are conducted to evaluate the effect of Active Flap on hover and forward flight performances. The hover analysis demonstrates that the required rotor power is reduced by 2.5 % with the positive 0/rev (quasistatic) flap deflection, which twists the blade in the nose down direction to reduce the local angle of attack and the local drag. The required power for hover changes non-linearly with respect to the flap deflections because of the independent behaviors of C_M and C_L variations. In forward flight analysis, the Active Flap is controlled by 2/rev, 3/rev and ideal flap deflections. The 2/rev and ideal controls can reduce the required rotor power for forward flight by 4% resulting from suppressing the negative angle of attack on the advancing blade. Furthermore, ideal control results in lower rolling and pitching moments acting on the hub than other harmonics, thus it can reduce re-trim control which is required when blades are actively controlled and can prevent significant increase of pilot workload. A conceptual design study on the Active Flap system to realize the developed flexible control law is carried out based on the previous research activities which had demonstrated the sufficient achievements. The system consists of two flaps and two drive mechanisms to share aerodynamic loads and prevent force fighting between the drive mechanisms.

1. INTRODUCTION

The rotorcraft is operated on a wide variety of flight conditions from hovering to high speed cruising, each of which inflicts the unique aerodynamic environment on the rotors, intrinsically to be coped with unique blade pitch control laws optimized for each flight condition. On the other hand, the current blade pitch control system of the rotorcraft using the swashplate mechanism can only make use of the collective pitch (0/rev) and the cyclic pitch (1/rev) due to mechanical limitations. This means that current blade pitch control system does not fulfill the required performance for each flight condition, but compromises within its capability.

If the flexible control systems are realized, there must be the great possibilities to develop the optimized blade pitch control system consisting of control laws and corresponding hardware for the various flight conditions with the wide speed range.

In this study, the flexible control is defined as the active blade pitch control systems which enable the blades to have not only conventional 0/rev and 1/rev pitch changes but also the quasistatic and 2/rev and higher harmonics in order to generate the optimal blade pitch change appropriate for each flight condition.

The quasistatic means that the Active Flap or the active twist is deflected and holds the deployment static, which can change the aerodynamic effect of the build-in twist by adjusting lift distribution along the blade.

The hardware candidates are HHC (Higher Harmonic Control) which drives the entire blade from the non-rotation frame, IBC (Individual Blade

Control) which also drives the entire blade but from the rotation frame, Active Twist which can twist the blade by actuator sheets installed inside the blade and Active Flap which also twists the blade but by a flap installed at the trailing edge of the blade tip region. They have been intensively and comprehensively researched and developed to reduce noise and vibration and to improve flight performances of rotorcraft[1]-[6].

Among those candidate active techniques for the flexible control system, Active Flap and Active Twist are more feasible than the others, especially considering the hover performance improvement. The induced power is dominant during hovering and can be effectively reduced by making the downwash as uniform distribution over the rotor disk as possible, which can be achieved by the quasistatic deployment of these two active techniques adjusting local twist, subsequently local lift and consequently downwash distribution along the blade. In an analytical study, it is shown that the quasistatic deployment of Active Twist achieved 10% reduction of the required hovering power at $C_T/\sigma=0.092$[7].

For improving the forward flight performance, the compressibility alleviation on the advancing side of the blade and/or the stall avoidance on the retreating side, where the adverse aerodynamic phenomena generate a large drag, should be achieved, hopefully, simultaneously. The wind tunnel test and analytical results with appropriate application of 2/rev blade pitch deflection by IBC demonstrated that the required power for the forward flight at $\mu=0.4$ is reduced by 5% by adjusting the local angle of attack distribution on the advancing side[8]. An analytical study with 2/rev Active Flap input demonstrated that the required power for the forward flight was reduced and the maximum speed is increased by suppressing the stall on the retreating side[9].

This study selects Active Flap technique as the flexible control system, because the authors' organizations have an abundant experience on this technique[10]-[14]. In the first step, this study analytically pursues and evaluates the control laws for improving the flight performance on the conditions of hover and forward flight using CAMRAD II[15]. In the next step, a conceptual design study on the Active Flap system to realize the developed flexible control law is considered based on the past and on-going Active Flap research activities.

2. ANALYTICAL METHOD

2.1. Overview

The influences of Active Flap control laws for flight performance are investigated using CAMRAD II; comprehensive analytical model of rotorcraft aerodynamics and dynamics.

The analyses for hover and forward flight are conducted using main rotor model with active trailing edge (T.E.) flaps based on the UH-60[10].

2.2. Analytical model

The parameters of analytical model are shown in Table 1 and blade geometry is shown in Figure 1. The aerodynamic blade elements are defined from r/R = 0.1925 to r/R = 1.0000. Chord length are constant, c = 0.5273 m, for all blade elements.

Table 1: Parameters of analytical model

Parameters	Value
Number of Blades	4
Rotor radius R [m].	8.178
Chord length c [m].	0.5273
Swept back region	0.94R - 1.0R
Swept back angle [deg].	20
Rotational speed [rpm]	258
T.E. flap region	0.7R - 0.8R
T.E. flap span	0.1R
T.E. flap chord	0.1c

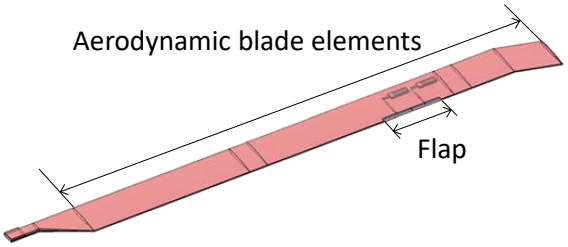

Figure 1: Blade geometry

2.3. Analytical conditions

The trim conditions for hover analysis are shown in Table 2. In hover analysis, high C_T/σ is selected so that the effect of T.E. flaps can be clearly observed.

In forward flight, the analysis is conducted at 160 kt, the maximum horizontal speed of UH-60, with the trim conditions shown in Table 3. The lift is selected with reference to the 1G weight of the UH-60 (20700 Lb)[16]. The drag is selected with reference to the airframe drag area of UH-60 (22 ft^2)[17].Since the analytical model consists of the isolated main rotor, the tip-path plane (TPP) is assumed to be perpendicular to the rotor shaft, and the thrust direction is changed according to the main rotor shaft angle.

Table 2: Trim Conditions for hover analysis

Trim target	Value
C_T/σ	0.16

Table 3: Trim Conditions for forward flight analysis

Trim target	Value
Lift [N].	92110
Drag area [m^2].	2
Longitudinal TPP tilt [deg].	0
Lateral TPP tilt [deg].	0

T.E. flap deflection is given by the sum of n/rev cosine waves as shown in equation (1), where A_n is the amplitude (deg) of the n/rev component, ψ is the azimuth angle (deg), and Φ_n is the phase angle (deg) of the n/rev component. The flap deflection is positive for trailing edge down and negative for trailing edge up as shown in Figure 2.

For hover, flap deflection is controlled using only 0/rev component. For forward flight, flap deflection is controlled using the 0 - 3/rev components.

(1) $$\delta_{TE} = A_0 + A_1 cos(\psi + \phi_1) + A_2 cos(2\psi + \phi_2) + \ldots + A_n cos(n\psi + \phi_n)$$

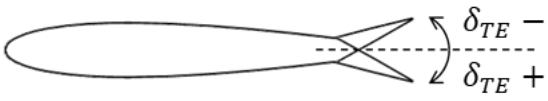

Figure 2: Definition of T.E. flap deflection

3. ANALYTICAL RESULTS

3.1. Hover analysis

3.1.1. Required power for hover

The required power with respect to 0/rev (quasistatic) flap deflection in hover analysis is shown in Figure 3. The required power for hover decreases with positive flap deflection (trailing edge down) and increases with negative flap deflection (trailing edge up). At a flap deflection of +8 deg, required power for hover becomes the lowest, which is about 2.5% lower than the power at a flap deflection of 0 deg. At positive flap deflection, required power for hover varies slightly. Therefore, required power for hover is sufficiently reduced even at small positive flap deflections.

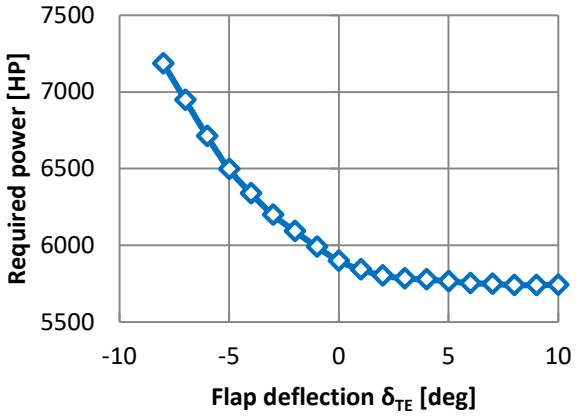

Figure 3: Required power with respect to 0/rev (quasistatic) flap input (Hover)

3.1.2. Mechanism to improve hover required power

The mechanism to improve hover required power is explained by the variations of aerodynamic coefficients with respect to T.E. flap deflection. Figure 4 shows spanwise effective angle of attack distributions at flap deflections of 0, +5 and -5 deg. At positive flap deflection, angle of attack decreases across the entire blade, and significantly decreases across the flap region.

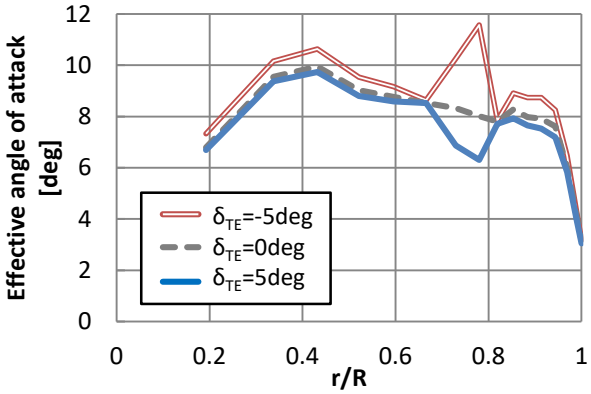

Figure 4: Spanwise effective angle of attack distributions (Hover)

Drag coefficients C_D and lift coefficients C_L at flap region (r/R=0.78) change with flap deflections as shown in Figure 5 and Figure 7, respectively. The curves of aerodynamic coefficients are illustrated by solid lines, and the values of aerodynamic coefficients at each flap deflections are indicated by symbols. The symbols are plotted at corresponding effective angle of attack to each flap angles, which are obtained from Figure 4.

At positive flap deflection, C_D decreases as the effective angle of attack decreases as shown in Figure 5. Therefore, drag decreases at positive flap deflection as shown in Figure 6. This suggests that the decrease of effective angle of attack with T.E. flap contributes the improvement of required power.

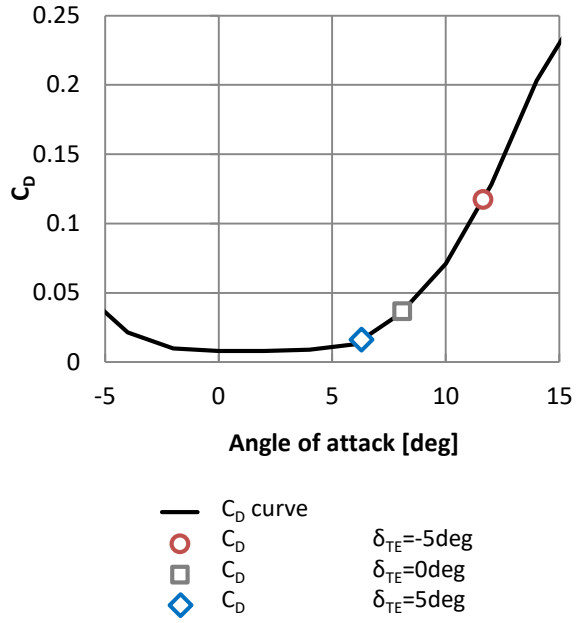

Figure 5: C_D with respect to flap deflection (Hover, r/R=0.78)

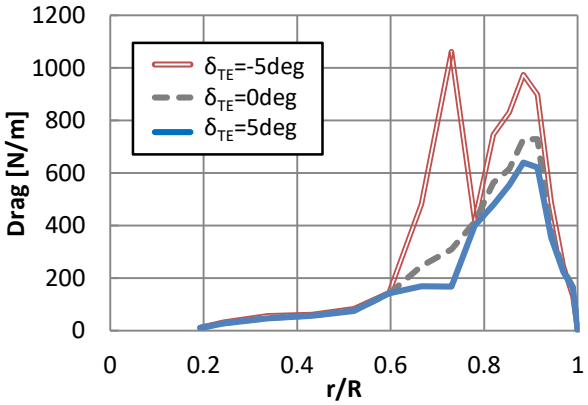

Figure 6: Spanwise local drag distributions (Hover)

C_L curve is shifted to higher at positive flap deflection as shown in Figure 7. Although the angle of attack decreases at positive flap deflection, because of shifted C_L curve, C_L at flap deflection of 5 deg is higher than C_L at lower flap deflections. Therefore, at positive flap deflections, blades can generate sufficient lift even with small angle of attack. The actual local lift distributions are shown in Figure 8. At positive flap deflection, lift at flap region (r/R=0.7 - 0.8) increases because C_L increases and lift outside flap region decreases because angle of attack decreases.

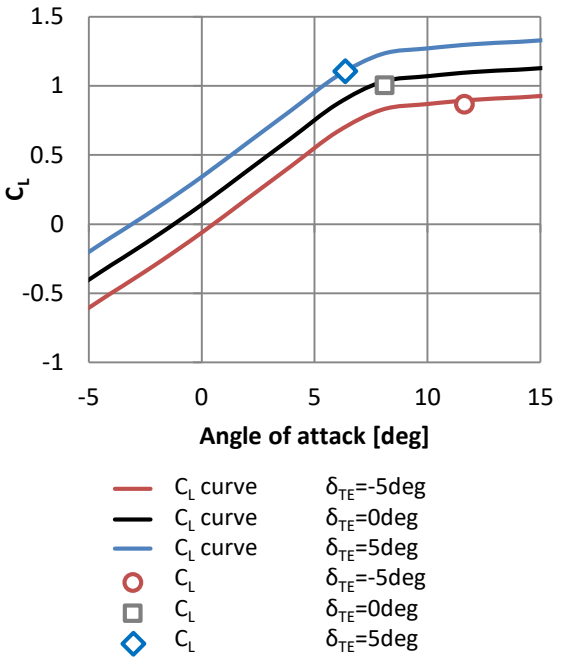

Figure 7: C_L with respect to flap deflection (Hover, r/R=0.78)

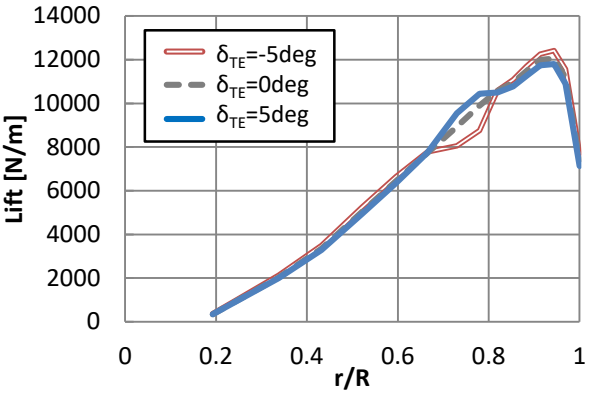

Figure 8: Spanwise local lift distributions (Hover)

Figure 9 shows trimmed CP angles with 0/rev flap deflections. At both flap deflections of +5 deg and -5 deg, trimmed CP angles increases compared to at 0 deg. To evaluate the reasons for this and the details how angle of attack changes, additional analysis with constant CP angle is conducted. CP angle is fixed to trimmed CP angle at flap deflection of 0 deg. Figure 10 to Figure 14 shows C_M, induced velocity, effective angle of attack, C_L and C_T/σ at constant CP angle at the flap (r/R=0.78). Considering these, the process how effective angle of attack and required power

change with respect to flap is considered as follows.

As shown in Figure 10, when the flap deflection is positive, the C_M decreases and becomes negative, thus blades are twisted in the nose down direction. In addition, the induced velocity increases as shown in Figure 11 and the effective angle of attack decreases as shown in Figure 12. On the other hand, C_L increases as shown in Figure 13, however, angle of attack decreases with respect to C_M, resulting in a decrease of C_T/σ as shown in Figure 14. Thus, at positive flap deflection, thrust is mainly changed by the deflection of blade pitch angle; T.E. flaps operate in servo-flap mode. In order to trim C_T/σ, CP angle increases. In trimmed condition, the decrease in effective angle of attack with respect to C_M and downwash is greater than the increase in effective angle of attack with respect to CP. Therefore, the effective angle of attack and the drag decreases, as a result, the required power decreases as shown in Figure 3.

As shown in Figure 10, when the flap deflection is negative, C_M increases and becomes positive, thus blades are twisted in the nose up direction. In addition, the induced velocity decreases as shown in Figure 11 and the effective angle of attack increases as shown in Figure 12. However, C_L decreases as shown in Figure 13, resulting in a decrease of C_T/σ as shown in Figure 14. Thus, at negative flap deflection, thrust is mainly changed by the deflection of C_L; T.E. flaps operate in direct-lift mode. To trim C_T/σ, CP angle increases. In trimmed condition, C_M, downwash by flaps, and CP change to increase the effective angle of attack. Therefore, the effective angle of attack and the drag increase, as a result, the required power increases as shown in Figure 3.

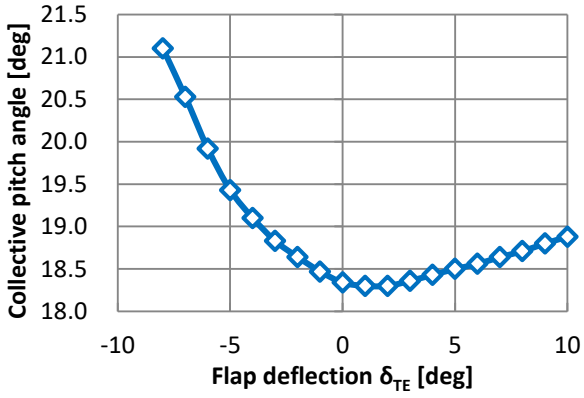

Figure 9: Collective pitch with respect to flap deflection

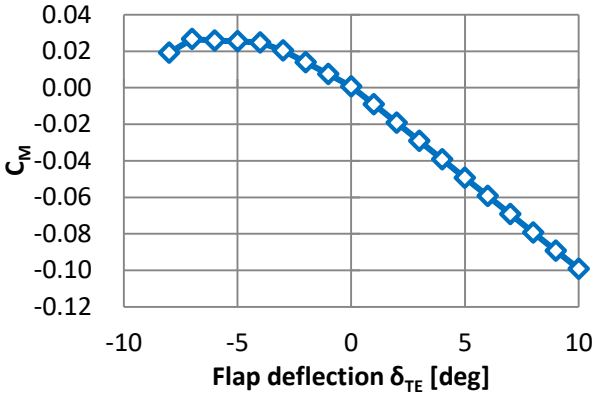

Figure 10: C_M with respect to flap deflection (Hover, constant CP, r/R=0.78)

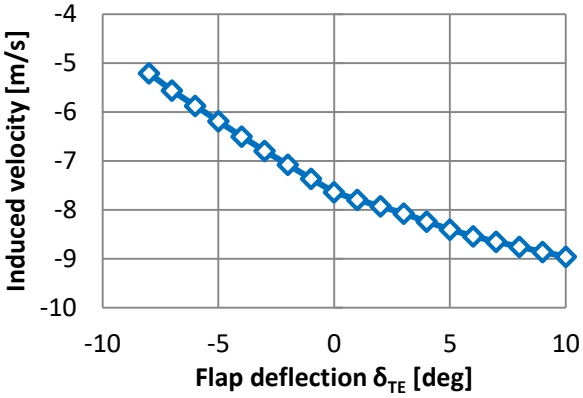

Figure 11: Induced velocity with respect to flap deflection (Hover, constant CP, r/R=0.78)

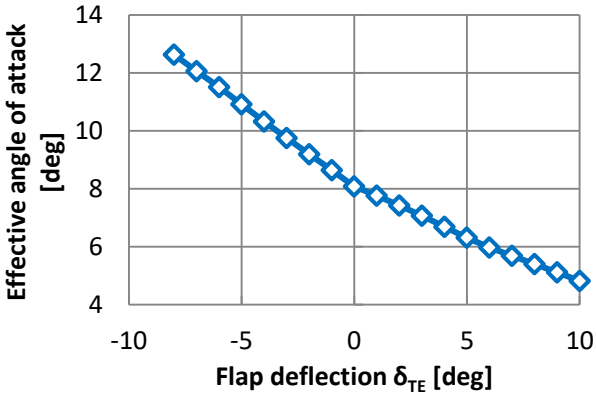

Figure 12: Effective angle of attack with respect to flap deflection (Hover, constant CP, r/R=0.78)

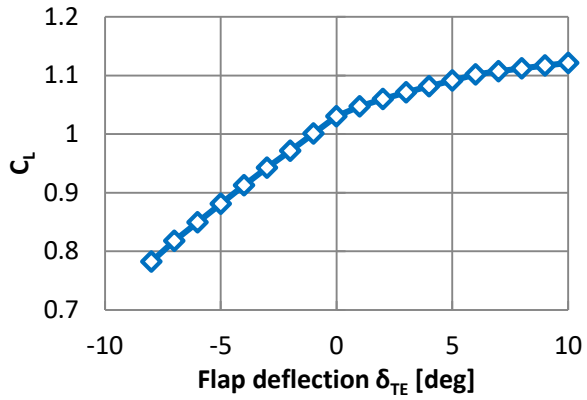

Figure 13: C_L with respect to flap deflection (Hover, constant CP, r/R=0.78)

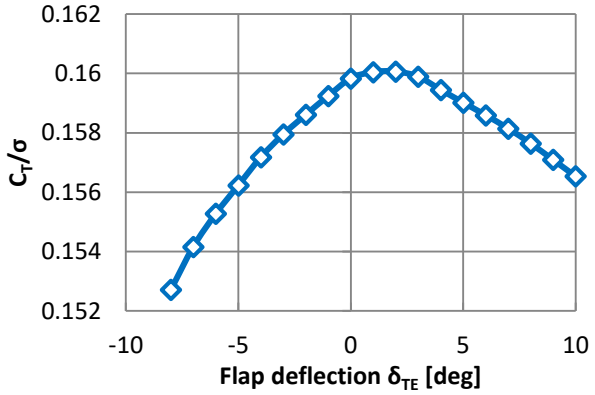

Figure 14: C_T/σ with respect to flap deflection (Hover, constant CP, r/R=0.78)

3.2. Forward flight

3.2.1. The definition of Active Flap input

Figure 15 and Figure 16 shows effective angle of attack and drag distribution at 160 kt (μ = 0.37) with flap deflection of 0 deg. (Hereafter, this case is referred to as passive case). In passive case, the effective angle of attack is negative and the drag is quite large on the advancing side. Therefore, it is necessary to reduce the absolute value of the negative angle of attack on the advancing side in order to reduce the required power.

Figure 17 shows the required power with respect to 2/rev and 3/rev Active Flap input phase. The required power is minimized at phase of 330 deg for 2/rev and at phase of 225 deg for 3/rev. The waveforms of flap input at the minimum required power are shown in Figure 18. At an azimuth angle of 105 deg, the flap deflection is negatively maximized (trailing edge up) for both 2/rev and 3/rev, which reduce negative angle of attack on the advancing side.

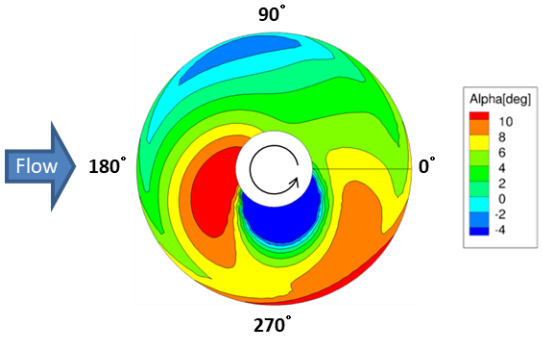

Figure 15: Effective angle of attack distribution (v=160 kt, Passive)

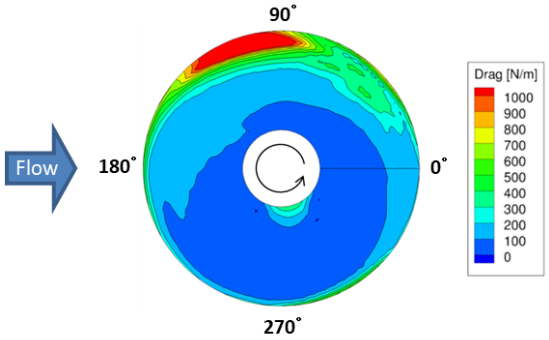

Figure 16: Drag distribution (v=160 kt, Passive)

However, as described later in 3.2.4, with 2/rev and 3/rev flap inputs, trimmed condition changes significantly and the pilot's workload can be significantly increased in the case of real flights. Therefore, in order to reduce the amount of re-trim control, the “ideal” flap control is investigated. The waveform of ideal flap control is induced from the effective angle of attack and drag distribution shown in Figure 15 and Figure 16, and actual flap input is formulated in Fourier series consisting of 0/rev to 3/rev harmonics. The red line in Figure 18 shows ideal flap control, and the ideal waveform is expressed by equation (2).

$$\delta_{TE} = 0.02 + 2.16\cos(\psi + 64.3) + 1.23\cos(2\psi + 329.3) + 1.33\cos(3\psi + 214.6) \quad (2)$$

Table 4 summarizes the frequencies, amplitudes and phases of each Active Flap input for forward flight. The influences of these Active Flap input for forward flight performance are compared through the analysis.

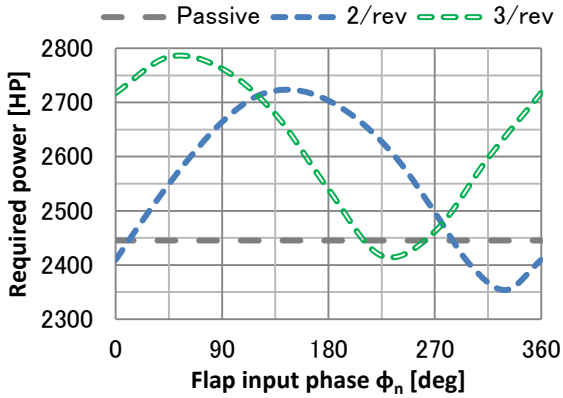

Figure 17: Required power with respect to flap input phase

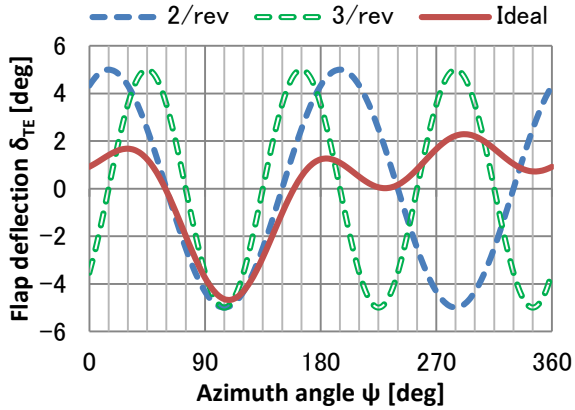

Figure 18: Waveform of Active Flap input

Table 4: Specifications of Active Flap input wave

	2/rev	3/rev	Ideal
Frequency	2/rev	3/rev	0 to 3/rev
Amplitude [deg].	5	5	Equation (2)
Phase [deg].	330	225	Equation (2)

3.2.2. Required power for forward flight

Figure 19 shows the required power for forward flight at 160 kt with each Active Flap input. With 2/rev and ideal input, the required power for forward flight at 160 kt can be reduced by about 4% compared to with passive case. With 3/rev input, the required power for forward flight at 160 kt is less reduced than with other harmonics though 3/rev input is also set to reduce negative angle of attack on the advancing side similarly to 2/rev and ideal input.

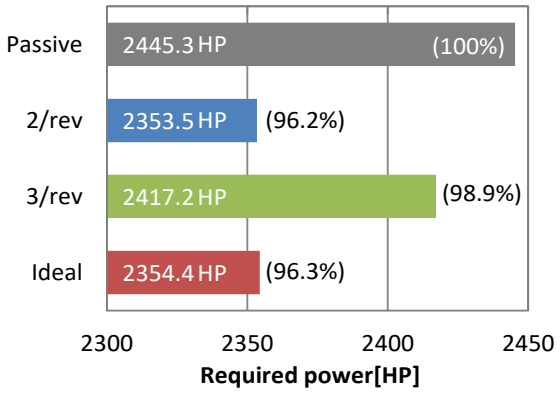

Figure 19: Comparison of required power with Active Flap input (v=160 kt)

3.2.3. Comparison of in-plane distribution

The in-plane distributions of effective angle of attack, lift and drag for each flap input cases are shown in Figure 20.

The negative angle of attack is suppressed and drag decreases on the advancing side for all Active Flap input cases. For 2/rev input case, drag on the advancing side decreases more than the other cases, while drag on the retreating side increases. This is because flap takes the same angles every 180 degrees for 2/rev and every 120 deg for 3/rev as described in equation (1), thus the angle of attack increases not only on the advancing side but also on the retreating side. On the other hand, for ideal input case, drag on the advancing side is less reduced compared to other cases, but drag does not increase on the retreating side because the flap deflection changes only on the advancing side.

3.2.4. Trim result

Table 5 shows the trimmed control, attitude and hub moment. Figure 21 shows the differences in trim results relative to passive case.

The coupling of Active Flap input and forward flight speed changes the trim results. According to Ref. [18], during active control at n/rev, the blade thrust varies at n-1/rev and n-2/rev not only at n/rev. Therefore, trimmed conditions is different because the 0/rev (collective) and 1/rev (cyclic) components are changed by active control at 2/rev and 3/rev. For ideal input, the rolling moment increases because of the drag reduction and the lift increase on the advancing side, but less increases than that of 2/rev and 3/rev because the flap deflection changes only on the advancing side. Therefore, ideal input is the best in terms of reducing the hub moment.

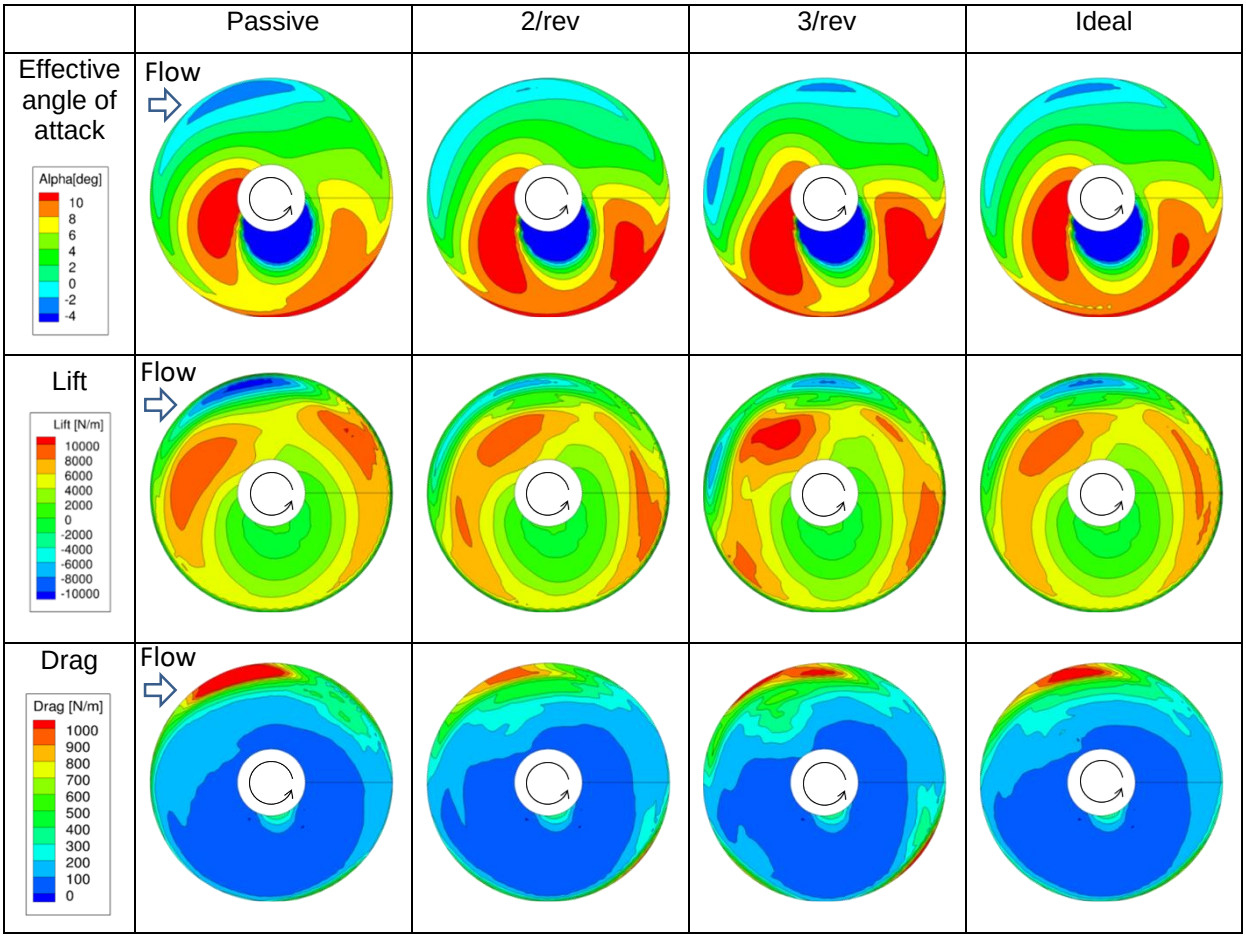

Figure 20: Distributions of effective angle of attack, lift, drag (v=160 kt)

Table 5: Trimmed control, attitude, and moment

	Passive	2/rev	3/rev	Ideal
Collective pitch [deg]	12.22	12.41	15.05	12.14
Longitudinal cyclic pitch [deg]	-3.23	-3.64	-3.87	-3.57
Lateral cyclic pitch [deg]	6.46	7.08	7.75	6.92
Airframe pitch angle [deg]	-7.21	-6.99	-9.40	-6.97
Rolling moment [N-m]	8179	8330	9350	8227
Pitching moment [N-m]	4669	4878	6505	4812

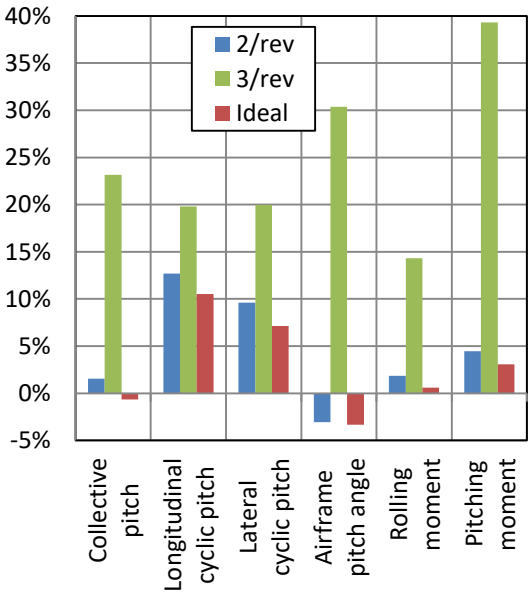

Figure 21: Differences of trim results for each flap input

3.2.5. Forward speed improvement

Forward speed improvement with Active Flap input is estimated based on the required power for 160 kt forward flight in passive case. Figure 22 shows the required power with respect to forward speed. 2/rev input and ideal input increases the forward speed by 3 kt compared to passive case.

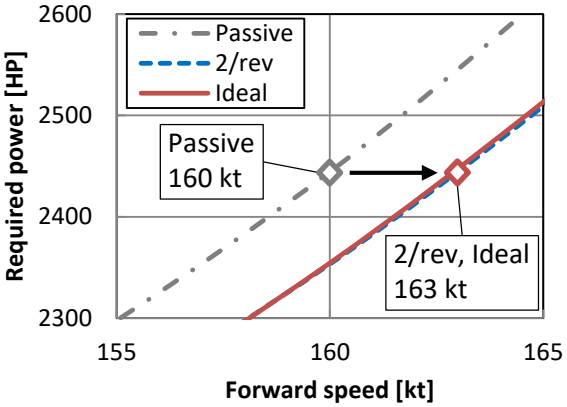

Figure 22: Required power with respect to forward speed (v=160 kt)

4. CONTROL SYSTEM DESIGN

4.1. Requirements for control system

From flap input waveform and T.E. flap hinge moment, the required specifications of the control system are set as shown in Table 6. Figure 23 shows T.E. flap hinge moments with respect to azimuth angle for forward flight with each Active Flap input. Figure 24 shows T.E. flap hinge moment with respect to flap deflection for hover with 0/rev (quasistatic) flap input.

Table 6: The required specifications for Active Flap

Status	Hover	v=160 kt
Input	0/rev	Ideal
Flap deflection [deg]	4.0	4.7
Operating speed [deg/s]		202
Inertial load [kg-m^2]		1.63×10^{-4}
Aerodynamic load [N-m]	0.9	1.9

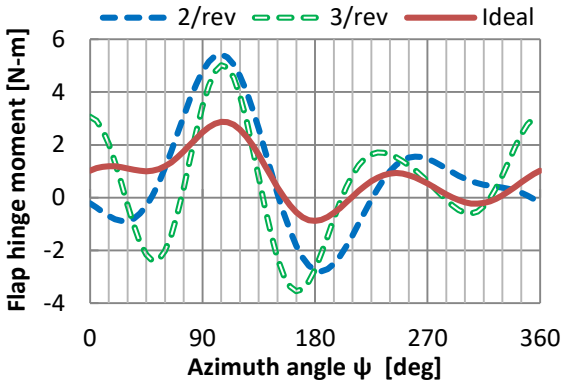

Figure 23: Flap hinge moment (v=160 kt)

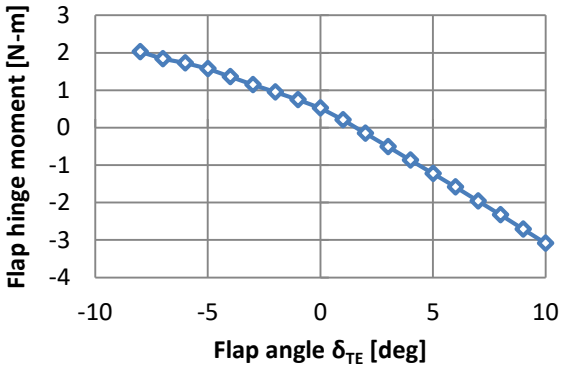

Figure 24: Flap hinge moment (Hover)

4.2. Active flap drive mechanism configuration

The configuration of the Active Flap drive mechanism is compared with the predecessor[10]-[14], which had been previously designed, prototyped and demonstrated the sufficient achievement by whirl tower test. The applicability of the same drive mechanism to the present study is examined. The comparison results are shown in Table 7.

As shown in Table 7, the Active Flap in this study needs 1.87 times larger control surface area and has to withstand 1.9 times larger aerodynamic load than the predecessor. While, as for the flap deflection, the required travel is 1.3 °less for both the positive and down sides.

Table 7: Active flap comparison

Item	Previous	This study
Surface area [m^2]	0.0232	0.0432
Flap deflection [deg]	±6	±4.7
Aerodynamic load [N-m]	1	1.9

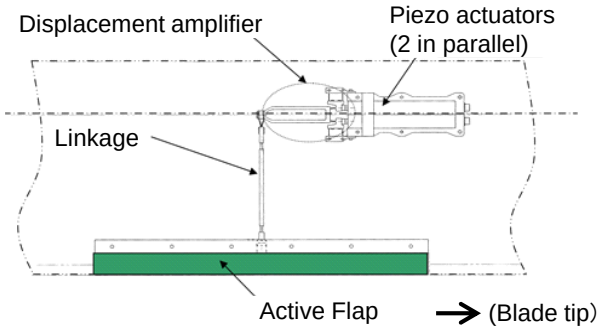

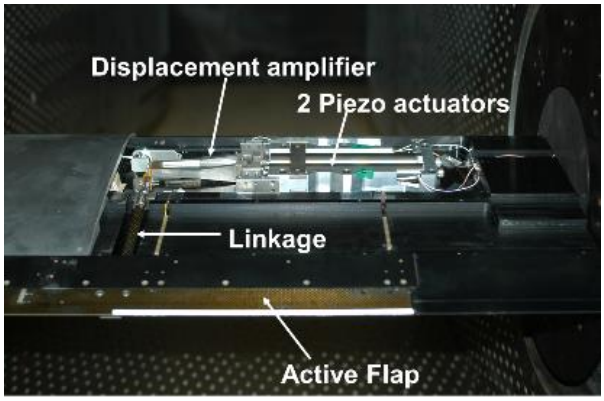

Figure 25: Drive mechanism (1 set)[18]

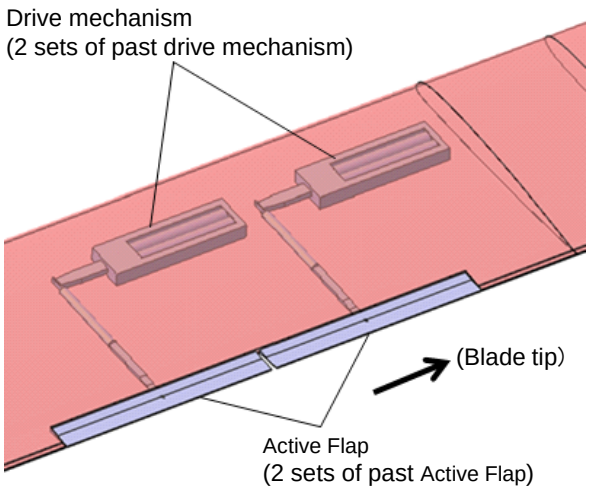

Figure 26: Active flap and drive mechanism

The increased size of the control surface area and the aerodynamic load can be handled by configuring a new drive mechanism with the two drive mechanisms in the previous case. Figure 25 shows the previous configuration with single drive mechanism. Figure 26 shows the new configuration adopting the two drive mechanisms.

As shown in Figure 26, in new configuration, the independent two flaps are prepared to avoid a force fight, which can be caused when there is a difference in output between two drive mechanisms which are connected parallel to operate one same flap. If force fight occurs, flaps become inoperative and the drive mechanism damage may occur.

4.3. The specification of Active Flap

Table 8 summarizes the specification requirements for the Active Flap and drive mechanism that meet the requirements for the Active Flap given in section 4.1 and adopting the configuration given in section 4.2.

The properties of the commercial piezo actuators which KHI used in the previous case are used in order to set the specification. The dynamic characteristics are set at a rotor speed of 258 rpm for the maximum frequency component (3/rev) included in the Ideal waveform.

Table 8: Specification of Active Flap (per blade)

Item	Value
Flap deflection [deg]	±5 MINIMUM
Actuator Stroke [mm]	0.26 MINIMUM *1
Operating Frequency [Hz]	12.9
Actuator Output [N]	12000 per actuator Total 4 actuator on one blade
Operating Voltage [VAC]	115 *2
Operating Current [A]	Max 0.8 per actuator *2 Total 4 actuator on one blade

**1. In Table 6, the flap deflection angle is required as ±4.7 deg minimum. Based on the previous experience, the flap deflection angle in this table is set as ±5 deg MINIMUM to have some margin. In the previous case, KHI designed the Active Flap deflection angle as ±6 deg MINIMUM.*

**2. Those values are based on the properties of the commercial amplifier of the piezo actuators which KHI used in the previous case. The maximum value of the operating current is set to the value same as the fuse rating of the amplifier.*

5. CONCLUSIONS

In order to improve hover and forward flight performance, the influence on performance of Active Flap is investigated by CAMRAD II analysis. In addition, required specifications of control system are estimated by analyzing results, and control

system which satisfies the requirements is designed. A summaries of conclusions are below.

Hover analysis

- The influence of 0/rev (quasistatic) flap deflection on hover performance is investigated and the required power for hover is reduced by about 2.5% with positive flap deflection (trailing edge down). Because the positive flap deflection makes the blade pitch down and drag is reduced by decreasing the angle of attack.
- The flap deflection changes C_M and C_L individually, resulting in the required power for hover changes non-linearly with respect to flap deflections.

Forward flight analysis

- The influence on forward flight performance is investigated for 2/rev, 3/rev, and ideal flap input. Ideal flap input focuses on reducing drag on advancing side.
- 2/rev and ideal flap input can suppress negative angle of attack on the advancing side. As a result, the required power at 160 kt is reduced by about 4%, which is equivalent that the forward speed can be increased by about 3 kt compared to the passive case.
- For ideal input, the rolling moment increases because of the drag reduction and the lift increase on the advancing side, but less increases than that of 2/rev and 3/rev because the flap deflection changes only on the advancing side.
- Ideal flap input shows the best results in terms of both required power and hub moment.

Control Systems

- The requirements for Active Flaps that can realize the ideal waveforms are set.
- The Active Flap drive mechanism is studied based on the previous research activities which had demonstrated the sufficient achievements. Since the flap area is large, two sets of drive mechanisms are used. The flap is divided into two sections to reduce the force fight.
- Using the drive mechanism examined, the specifications of the active flap satisfying the required specifications are set including the actuator specifications.

6. FUTURE WORKS

In order to improve the performance by Active Flaps and to develop a more efficient control system, the following issues are considered.

Forward flight analysis

- Optimization of ideal waveform (combination of frequency, amplitude, and phase in Equation (1)).

Control Systems

- Detailed study of a more efficient mechanism to drive the flap.

REFERENCES

[1] K. Nguyen, I. Chopra, “Application of Higher Harmonic Control to Hingeless Rotor Systems”, NASA Technical Memorandum 103846.

[2] K. Nguyen, “Higher Harmonic Control Analysis for Vibration Reduction of Helicopter Rotor Systems”, NASA Technical Memorandum 103855.

[3] K. Nguyen, M. Betzina, C. Kitaplioglu, “Full-Scale Demonstration of Higher Harmonic Control for Noise and Vibration Reduction on the XV-15 Rotor”, American Helicopter Society 56th Annual Forum, Virginia Beach, VA, May 2-4, 2000.

[4] W. R. Splettstoesser, K. –J. Schultz, B. van der Wall, H. Buchholz, “Helicopter Noise Reduction by Individual Blade Control (IBC) – Selected Flight Test and Simulation Results -“, the RTA – AVT Symposium, Braunschweig, Germany, May 8-12, 2000.

[5] D. Douglas Boyd, Jr., “Initial Aerodynamic and Acoustic Study of an Active Twist Rotor Using a Loosely Coupled CFD/CSD Method”, 35th European Rotorcraft Forum, Hamburg, Germany, September 22-25, 2009.

[6] L. Liu, D.Patt, P. Friedmann, “Simultaneous Vibration and Noise Reduction in Rotorcraft Using Aeroelastic Simulation”, American Helicopter Society 60th Annual Forum, Boltimore, MD, June 7-10, 2004.

[7] M. W. Floros, W. Johnson, “Advanced Rotor Aerodynamics Concepts with Application to Large Rotorcraft”, American Helicopter Society Aerodynamics, Acoustics, and Test and Evaluation Technical Specialists Meeting, San Francisco, CA, January 23-25, 2002.

[8] H. Yeo, E. A. Romander, T. Norman, “Investigation of Rotor Performance and Loads of a UH-60A Individual Blade Control System”, American Helicopter Society 66th Annual Forum, Phoenix, Arisona, May 11-13, 2010.

[9] A. Altmikus, A. Dummel, R. Heger, D. Schmke, “Actively Controlled Rotor: Aerodynamic and Acoustic Benefit For The Helicopter Today And Tomorrow”, 34th European Rotorcraft Forum, Liverpool, UK, September, 2008

[10] Kobiki, N., Yamakawa, E., Hasegawa, Y., Okawa, H., “Aeroelastic Analysis and Design for On-blade Active Flap”, 25th European Rotorcraft Forum, Rome Italy, 1999.

[11] Hasegawa, Y., Katayama, N., Kobiki, N., Yamakawa, E., “Whirl Test Results of ATIC Full Scale Rotor System”, 26th European Rotorcraft Forum, The Hague, The Netherlands, 2000.

[12] Hasegawa, Y., Katayama, N., Kobiki, N., Nakasato, E., Yamakawa, E., Okawa, H., “Experimental and Analytical Results of Whirl Tower Test”, 57th Annual Forum of the American Helicopter Society, Washington, DC, May, 2001.

[13] Kobiki, N., Saito, S., Fukami, T., Komura, T., “Design and Performance Evaluation of Full Scale On-board Active Flap System”, 63rd Annual Forum of American Helicopter Society, Virginia Beach, VA, May 1-3, 2007.

[14] Kobiki, N., Saito, S., “Performance Evaluation of Full Scale On-board Active Flap System in Transonic Wind Tunnel”, 64th Annual Forum of American Helicopter Society, Montreal, Canada, April 29-May 1, 2008.

[15] W. Johnson, “ROTORCRAFT AEROMECHANICS APPLICATIONS OF A COMPREHENSIVE ANALYSIS”, AHS International Meeting on Advanced Rotorcraft Technology and Disaster Relief, Japan, April 1998.

[16] S. Jon Davis, “Predesign Study For a Modern 4-Bladed Rotor For The RSRA”, NASA-CR-166155,1981.

[17] H. Yeo, W. G. Bousman, W. Johnson, “Performance Analysis of a Utility Helicopter with Standard and Advanced Rotors”, Journal of the American Helicopter Society, 2004, 49, pp. 250-270.

[18] Kobiki. N., “JAXAにおけるヘリコプタ騒音低減用アクティブ技術の研究 (Research of active control technique for helicopter noise reduction in JAXA)”, Journal of the Japan Chapter of AHS International, Vol. 23, July 2013, pp.92-93, http://www.helijapan.org/pdf/general/general108/Fy2013JHS-kaihou.pdf.